Title

Marine biodiversity refugia in a climate-sensitive subarctic shelf

Running title

Contemporary marine biodiversity refugia

Authors

Irene D. Alabia[1*], Jorge García Molinos[1,2,3], Takafumi Hirata[1,3], Franz J. Mueter[4], Toru Hirawake[5], and Sei-Ichi Saitoh[1]

[1]Arctic Research Center, Hokkaido University, 001-0021 Sapporo, Japan

[2]Global Station for Arctic Research, Global Institution for Collaborative Research and Education, Hokkaido University, Sapporo, Japan

[3]Graduate School of Environmental Science, Hokkaido University, Sapporo, Japan

[4] College of Fisheries and Ocean Sciences, University of Alaska Fairbanks, Juneau Alaska, United States of America

[5]Faculty of Fisheries Sciences, Hokkaido University, 041-8611 Hakodate Japan

Correspondence: irenealabia@arc.hokudai.ac.jp

Abstract

The subarctic shelf of the Eastern Bering Sea (EBS) is one of the world's most productive marine environments, exposed to drastic climate changes characterized by extreme fluctuations in temperature, sea ice concentration, timing, and duration. These climatic changes elicit profound responses in species distribution, abundance, and community composition. Here, we examined patterns of alpha- and temporal beta-diversity of 159 marine taxa (66 vertebrates and 93 invertebrate species) from 29 years (1990-2018) of species observations from the NOAA bottom trawl surveys in the EBS. Based on these data, we identified geographically distinct refugial zones in the northern and southern regions of the middle shelf, defined by high species richness and similarity in the community species composition over time. These refugial zones harbor higher frequencies of occurrence for representative taxa relative to the regions outside of refugia. We also explored the primary environmental factors structuring marine biodiversity distributions, which underpinned the importance of the winter sea ice concentration to alpha- and temporal beta-diversity. The spatial biodiversity distributions between high and low winter sea ice regimes highlighted contrasting signals. In particular, the latter showed elevated species richness compare to the former. Further, the temporal beta-diversity between the high and low winter sea ice periods underpinned an overall increase in the compositional similarity of marine communities in the EBS. Despite these spatio-temporal differences in biodiversity distributions, the identified refugia are safe havens of marine biodiversity in the EBS, and distinguishing these areas can help facilitate conservation and management efforts under accelerated and on-going climatic changes.

Key words: Eastern Bering Sea, alpha diversity, biodiversity refugia, temporal beta-diversity, sea ice, Pacific Arctic region

1. Introduction

Marine biological diversity encompasses all levels of complexity of life in the ocean, assumes multiple ecosystem functions, and provides a plethora of valuable ecosystem services (Sala and Knowlton, 2006; Cavanagh et al., 2016; Barbier, 2017). Understanding the temporal trends, spatial patterns, and forces structuring biodiversity are critical to bolstering conservation and resource management efforts under multiple climatic and ecological disturbances (Sala and Knowlton, 2006; Tittensor et al., 2010; Selig et al., 2014). In particular, climate-driven changes in the abiotic environment combined with pervasive anthropogenic threats have caused unprecedented impacts on global marine biodiversity, as manifested through population declines, species extirpation, and community shifts (Sala and Knowlton, 2006; Genner et al., 2010; Sydeman et al., 2015; Malhi et al., 2020).

The importance of conservation strategies and climate adaptation tools in reducing biodiversity losses along with their ecological and societal impacts is widely recognized. One of the increasingly proposed conservation approaches involves identification and protection of climate change refugia, which target regions that are resistant to on-going climatic changes relative to the surrounding environment (Keppel et al., 2012; Morelli et al., 2016). The concept of refugia was earlier introduced to explain species distributional patterns within the context of past climatic changes and characterized as locations where taxa may move to and persist during large-scale and long-term climatic changes (Keppel et al., 2012; Keppel et al., 2015). Hence, refugia provide a suite of spatio-temporal abiotic environments favorable for a given species and are especially crucial when the surrounding environmental conditions become inhospitable (Ashcroft, 2010; Stewart et al., 2010; Morelli et al., 2017). The identification of refugia over shorter, ecological time scales is being pursued within the perspective of biodiversity adaptation to recent anthropogenic climate changes (Morelli et al., 2017; Morelli et al., 2020). Within this context, climate change refugia are defined as habitats relatively buffered from the

contemporary climate change that permit the persistence of valuable physical, ecological, and socio-cultural resources (Morelli et al., 2016).

Multiple techniques to identify refugia have been explored and developed, often limited by the availability of climate and resource data. While most of these methods were predominantly applied to terrestrial and freshwater systems (Ashcroft et al., 2012; Isaak et al., 2016; Baumgartner et al., 2018), their use has been increasingly expanded to marine ecosystems. Earlier attempts to identify marine refugia were primarily focused on tropical coral reefs (Ban et al., 2012; Hooidonk et al., 2013). More recently, climate change refugia studies have progressed to accommodate broader ecological components of marine ecosystems. In particular, climate change refugia in both pelagic and shelf ecosystems have been identified based on the persistence of high genetic diversity (Provan, 2013; Assis et al., 2016), the resilience of diverse seascapes to environmental and climatic changes (Ban et al., 2016), and the occurrence of topographic features (Pinheiro et al., 2017; Kapsenberg and Cyronak, 2019) and oceanographic phenomena (Lourenço et al., 2016; Storlazzi et al., 2020). Another novel approach to identifying marine climate change refugia was through the use of in-situ species community observations in areas where long-term and consistent spatial biodiversity monitoring has been in place (Barceló et al., 2018). In this case, potential refugial zones are exemplified by regions that maintained high species richness and minimal change in the species composition over time. Invoking a multi-species community perspective to identifying refugia can further complement the limitation and trade-off of ecological niche models and taxon-specific approaches (Planque, 2016; Hollowed et al., 2000) for management applications and detecting potential locations of climate-resistant species communities (Barceló et al., 2018).

Here, we implemented a biodiversity-based approach (Barceló et al., 2018) for identifying biodiversity refugial zones in the EBS, which is among the most productive yet climatically-sensitive shelf ecosystems in the world (Overland and Stabeno, 2004). While

climate change refugia often represent biodiversity safe havens in the conservation planning literature (Keppel et al., 2012; Keppel et al., 2015), actual validation of whether these are indeed accrual areas for biodiversity is often overlooked (Barrows et al., 2020). Hence, we also compared biodiversity refugia to climatically stable areas (Ban et al., 2016) in the EBS shelf and examined their spatial correspondence, providing a potential independent validation of climate change refugia in this region (Barrows et al., 2020). We further examined the spatial and temporal patterns of alpha and beta diversity in the Eastern Bering Sea (EBS) in relation to environmental drivers between 1990 and 2018, a period characterized by large fluctuations in thermal and sea ice conditions. Over the past decades, the EBS has experienced pronounced environmental and climatic changes that elicited community-wide biological responses (Eisner et al., 2014; Duffy-Anderson et al., 2017; Stabeno et al., 2017). Thus, the primary objectives of this work are (1) to identify biodiversity refugial zones for marine species communities on the EBS shelf under contemporary climate changes; and (2) to examine recent spatio-temporal patterns of marine biodiversity and associated environmental drivers.

2. Methods

2.1 Study area

The study area is the Eastern Bering Sea shelf, situated in the Pacific sector of the Arctic (Fig. S1, inset map). This shallow continental shelf is one of the most fishery-productive and well-monitored marine areas in the world. The EBS is a wide (>500 km) continental shelf system, topographically classified by persistent fronts into the inner (<50 m water depth), middle (50–100 m), and outer (100–200 m) domains (Coachman, 1986). Each individual domain has its own unique hydrography, circulation, and species assemblages and food webs (Springer et al., 1996; Danielson et al., 2011; Hunt et al., 2011). The region further exhibits extremely high sensitivity and exposure to environmental and climatic changes (Stabeno et al., 2017; Stabeno and Bell, 2019). Particularly, the unprecedented warming and loss of seasonal sea ice cover on

the shelf over the recent decades have triggered pronounced impacts on productivity (Eisner et al., 2016; Duffy-Anderson et al., 2017) and on species abundances and distributions (Alabia et al., 2018; Stevenson and Lauth, 2019; Hirawake and Hunt, 2020).

2.2 Marine fish and invertebrate data

The biological data were sourced from the NOAA annual bottom trawl surveys between 1990 and 2018. While bottom trawl surveys were conducted from 1982, we started our analyses from 1990 to minimize the uncertainty from species identification in earlier years (Stevenson and Hoff, 2009). Summer (late May-August) bottom trawl surveys were annually conducted and covered up to 376 standard stations (Table S1) distributed across the sampling strata (Fig. S1) (Stauffer, 2004). Standard-density sampling strata have fixed stations in the center of the 20 x 20 nmi (37.04 x 37.04 km) cells while high-density strata encompass additional sites at the corners of the 20 x 20 nmi grids around the Pribilof and St. Matthew islands (Stauffer, 2004). Only commonly sampled taxa, defined as those recorded at one or more stations for at least 20 of the 29 years comprising the study period, were included in the biodiversity analyses (Table S2). This was done to minimize the potential bias from the inclusion of rare species in the calculation of diversity measures. This resulted in a total of 159 taxa comprising 66 largely demersal fish and 93 benthic invertebrate taxa belonging to three major taxonomic groups (Fig. S2). We included several typically pelagic species (Table S2, e.g. Pacific herring, capelin, and chum salmon) that were regularly caught in the bottom trawl. Invertebrates belonging to less represented phyla (n = 10) were combined into an ‘others’ group.

2.3 Alpha and beta-diversity metrics

Annual site-specific biodiversity metrics were calculated using species matrices based on presence-absence data derived from the raw species abundances (i.e., species presence records corresponding to abundances greater than zero). We used presence-absence species data over abundance-based species richness to reduce the confounding effect of density on compositional

similarity due to potential differences in sampling sizes (Jost et al., 2010). The annual alpha (α) diversity was then computed as the total number of species present at each survey site (i.e., species richness). Temporal beta-diversity was computed based on the Sorensen dissimilarity index computed between consecutive years at each site. For consecutive years with unsurveyed stations, temporal beta-diversity metrics were also set to missing values to ensure consistent analysis throughout the study period and avoid potential interpretation bias. We also utilized the Sorensen index for our analysis as it weighs matches in species composition between site pairs more heavily than mismatches thus, is more suitable for evaluating similarity in species-rich communities where some taxa could be absent in a given sample (Krebs, 2014). These year-to-year changes in community composition were calculated to capture the documented species and community–wide responses to inter-annual fluctuations of seasonal processes in the EBS (Baker and Hollowed, 2014; Ortiz et al., 2016). These include environmental (e.g. extent and retreat of sea ice) and biological processes (e.g. population dynamics, species growth, and recruitment). All biodiversity metrics were calculated using the 'betapart' package (version 1.5.1) (Baselga and Orme, 2012) in the R open source software (version 4.0.3).

2.4 Identifying biodiversity refugia for the marine fish and invertebrate community

Biodiversity refugia on the EBS shelf were identified as areas harboring high species richness and experiencing low compositional changes across the 29-year period (Barceló et al., 2018). Annual species richness data between 1990 and 2018 were averaged and standardized to range from 0 to 1. The compositional similarity was also computed as the inverse of the Sorensen index averaged over the period from 1991-2018. The refugia index was then computed as the product of the normalized alpha-diversity and compositional similarity measures (Barceló et al., 2018). The refugia index threshold for the identification of refugial zones was arbitrarily set to 0.31, representing the 90% quantile of the computed metric and the maximum cut-off value delineating the gradient between pixels of high and moderate refugia index.

166 **2.5 Local environmental data**

167 We compiled a preliminary pool of 14 environmental factors to explore their effects on marine
168 biodiversity facets in the EBS (Table S3). The datasets comprised in-situ observations of
169 bottom depth and bottom and surface temperatures collected during the bottom trawl surveys,
170 spatially-interpolated at 25 x 25 km spatial resolution using a nearest-neighbor gridding
171 algorithm implemented within the GMT software (Wessel et al., 2013). From the interpolated
172 in-situ data, annual spatial gradients of summer temperatures were then calculated using a 9-
173 pixel kernel neighbourhood with diagonal weighting (Burrows et al., 2011). The remaining
174 parameters were derived from satellite-based measurements of distance to the nearest coast
175 (https://oceancolor.gsfc.nasa.gov/docs/distfromcoast/, date accessed: 31 May 2018) at 0.04°
176 spatial resolution, seasonal averages of sea surface temperature (SST) and sea ice concentration
177 (SIC) from the daily NOAA OI SST V2 High Resolution dataset
178 (https://psl.noaa.gov/data/gridded/data.noaa.oisst.v2.highres.html, date accessed: 18 June
179 2018) at 25 x 25 km spatial resolution. The maximum, minimum, and average summer (May-
180 August) and winter (January-April) SST were calculated. For SIC data, we also computed for
181 winter average and pixel-wise persistence of sea ice cover, defined as the number of days where
182 a grid has a SIC value greater than 15% between February and September. Each environmental
183 parameter was averaged over similar consecutive years during which, the annual temporal beta-
184 diversity was computed. The fluctuations in seasonal sea ice dynamics and thermal conditions
185 in the EBS regulated recent trophic and biogeographic shifts (Mueter and Litzow, 2008; Alabia
186 et al., 2018). Finally, strongly correlated environmental variables ($r > 0.5$; Fig. S3) were
187 discarded to prevent problems with model identifiability (Tittensor et al., 2010).

188 **2.6 Identifying climatically stable areas**

189 We also identified climatically stable regions (sensu Ban et al., 2016) on the EBS shelf based
190 on sea ice concentration and seasonal (winter and summer) sea surface temperatures from

1990-2018. For each environmental variable, we computed pixel-wise anomalies from the corresponding 29-year average and performed a Mann–Kendall monotonic trend analysis (Abdi et al., 2019) (Fig. S4a-c). The results were then classified into equal quintiles to categorize the magnitude of climatic changes (large decrease, small decrease, largely unchanged, small increase, large increase) and identify areas of stability for each parameter (Ban et al., 2016) (Fig. S4d-e). Parameter-specific stable areas were selected as pixels in the middle quintile (largely unchanged/neutral pixels) and climatically stable regions were mapped as areas of overlapping stable conditions across the three environmental variables.

2.7 Environmental correlates with marine biodiversity

To examine the relationships between environmental parameters and alpha and beta-diversity in the EBS, we developed generalized additive mixed models (GAMMs) using environmental factors (n = 6) according to the following equation:

$$n_{i,t} = yr + s(x_i, y_i) + \sum g_k\left(EV_{i,t}^{k}\right) + \varepsilon_{i,t}$$

where $n_{i,t}$ is the observed response variable (either α- or temporal β-diversity) at station i sampled in year t, yr is a year-specific intercept, x_i and y_i are the longitude and latitude of station i, s is a two-dimensional thin-plate regression spline, g_k is a one-dimensional thin-plate regression spline fit to environmental variable EV^k measured at station i in year t, and $\varepsilon_{i,t}$ is a residual error that is assumed to have a Gaussian spatial autocorrelation structure to allow for year-specific random variations in the spatial patterns (Wood, 2006).

For each biodiversity metric, three models were constructed using different correlation structures (i.e. Gaussian, exponential, and spherical) to account for within-year variability in spatial patterns of the observed response variable among years. The best model was selected as the one with the highest proportion of deviance explained based on the adjusted coefficient of determination (Adj R^2) and lowest Akaike Information Criterion (AIC) (Table S4). Using

the best model, we then examined the significant partial effects of each environmental factor as well as spatial and temporal covariates (Fig. S5) to alpha and beta-biodiversity.

2.8 Marine biodiversity under contrasting winter sea ice regimes

We examined the spatial and temporal patterns of alpha diversity averaged across periods characterized by differences in mean winter sea ice concentration (wsic), as determined by the regime shift detection tool (Rodionov, 2006). The regime shift index was calculated using a 10-year cut-off regime length at a significance level of 0.05 to capture the decadal-scale climate variability in the EBS. Based on this analysis, our study duration constituted periods of high (hwsic: 1990-1999; 2008-2013) and low (lwsic: 2000-2007; 2014-2018) winter sea ice conditions in the EBS (Fig. S6).

Finally, we quantified species turnover and nestedness (Baselga, 2013) and identified indicator species (Cáceres and Legendre, 2009) for low-ice (13 years) and high-ice (16 years) regimes based on observed species abundances. Using station-specific species abundances by weight averaged across years within each of the wsic regimes, we computed the abundance-based temporal beta-diversity between hwsic and lwsic regimes based on the Bray-Curtis index (Baselga and Orme, 2012). The dissimilarity metric was partitioned into two components that account for balanced variation in abundance (turnover), whereby the abundance of some taxa in one site is replaced by an equal abundance of different species in another site; and unidirectional abundance gradients (nestedness), whereby the abundance of some species decreases from one site to the other (Baselga, 2013). Further, to quantify the relative species-specific contributions to the overall dissimilarity we conducted a similarity percentage analysis using the 'simper' function in the vegan package (version 2.5-6) in R (Oksanen et al., 2019). This function implements a pair-wise comparison of groups and computes the average contribution of each taxon to the compositional dissimilarity between two regimes. To identify indicator species associated with each regime we quantified regime affinity using a multi-level

pattern analysis based on the point biserial correlation index using the '*multipatt*' function of the indicspecies (version 1.7.7) R package (Cáceres and Legendre, 2009). The index evaluates the association between species and environmental conditions across the sampling sites based on the site-group combination with the highest difference between the species observed and expected abundance (De Cáceres et al., 2010).

3. Results

3.1 Temporal trends in marine biodiversity

Average local alpha and beta-diversity respectively increased (4 species richness/decade, $p < 0.001$) and decreased (-0.02 dissimilarity/decade) over time across the entire study region (Fig. 1). Overall, the downward trend in the temporal Sorenson dissimilarity was accounted for by a higher decline in the nestedness (-0.011 dissimilarity/decade, $p < 0.001$) relative to the turnover (-0.009 dissimilarity/decade, $p < 0.01$) component. Lower than average species richness and higher than average dissimilarity in community composition relative to the climatological means (across all years) were recorded until around 2000, then reversed for the rest of the series (Fig. 1). Nonetheless, there was high variability in the local annual alpha and beta-diversity. Notably, the temporal Sorensen dissimilarity showed higher variability across survey sites over the 29-year period.

3.2 Marine refugial zones on the EBS continental shelf

Spatial distributions of the alpha and temporal beta-diversity over the 29-year period showed salient patterns (Fig. 2) and captured potential refugial zones on the EBS continental shelf (Fig. 2c), exhibiting modest spatial correspondence with climatically stable regions (Fig. 2d, Fig. S4 d-f). The middle shelf (50-100 m) had the highest average species richness (Fig. 2a) and moderate to high species compositional similarity (Fig. 2b) over the 29-year period. Based on the combination of both parameters, two geographically-distinct and spatially contiguous biodiversity refugial zones (refugia index > 0.31) were identified: a north and south refugium

covering 21 and 16 survey stations, respectively (Fig. 2c). Both refugial areas were primarily defined by high species richness, but only the northern refugium had elevated compositional similarity over time. Spatial distributions of climatically stable regions also highlighted two distinct patches of moderate–high overlap across environmental variables and were spatially-extensive in the north than in the south portion of the middle shelf (Fig. 2d).

Fish taxa dominated taxonomically in both refugial zones by frequency of occurrence, particularly in the northern refugium where this group reached a total of 36 fish species (Fig. 3). Within the invertebrate group, mollusks and crustacean species represented the highest number in both refugial zones. Biogeographically, the north refugium accounted for a higher total number of species (78 taxa) relative to the south refugium (62 taxa). Out of the entire species pool (159), four taxa were equally present in both refugia while 15 species were absent in both refugia. Importantly, these refugial zones constitute only 7% of the entire study region but harbor 91% (n = 144) of the species pool, of which 50% (n = 79) had higher average frequencies across stations over the 29-year period inside than outside the refugia. In particular, 16 out of the 19 representative taxa were present at more stations and years inside than outside the refugia, with the majority (14/16) frequently occurring in the northern refugium (Table 1).

3.3 Environmental effects on marine biodiversity

Models of diversity explained a higher proportion of the total variance in alpha diversity (R^2 = 0.46) than in beta-diversity (R^2= 0.15). Whereas all environmental correlates had a statistically significant effect on alpha diversity, only four predictors (i.e., winter sea ice concentration, bottom depth, distance to coast, and bottom temperature gradient) had a significant association on beta-diversity (Table 2). Nonetheless, both models showed the highest significant effect of winter sea ice on marine biodiversity patterns in the EBS based on their F-values and statistical significance.

Response curves for significant environmental predictors captured the preferable ranges that were associated with higher regional marine biodiversity in the EBS (Fig. 4). In particular, bottom and surface temperature gradients had significant positive effects on alpha diversity at values closer to zero (Fig. 4a-b). In contrast, a moderate range of maximum summer SSTs (10-13°C; Fig. 4c), high winter sea ice concentration (wsic > 70%; Fig. 4d), deeper depths (60-120 m; bdep; Fig. 4e), and farther distances to the nearest coast (50-150 km; Fig 4f) were associated with higher alpha diversity. Meanwhile, the beta-diversity decreased with increasing bottom temperature gradient (Fig. 4g). It was also lowest in areas without winter sea ice but increased rapidly with increasing sea ice concentration and remained high over a broader range (20-95%; Fig. 4h) compared to alpha diversity. Beta-diversity increased with bottom depth, similar to yet more gradually than alpha diversity (Fig. 4i). In addition, distances farther away from the nearest coast had higher temporal beta-diversity (Fig. 4j).

3.4 Spatial distributions of marine biodiversity under contrasting sea ice regimes

Contrasting winter sea ice regimes in the EBS exhibited distinct patterns in alpha diversity distributions (Fig 5). Overall, species richness was substantially lower during the high sea ice regime (22.80 ± 2.75 species) compared to levels reached during low (25.83 ± 3.69 species) sea ice conditions (Fig. 5a-b). Pronounced changes in species richness between both regimes were observed across the middle and outer shelves and peaked at the southern part of the middle shelf, where local assemblages contained up to 10 species more during the low sea ice period (Fig. 5c).

In contrast, patterns in temporal beta-diversity suggest a high similarity in species composition between regimes over much of the area with the exception of the northeast middle domain (Fig. 6a). Locally elevated dissimilarity in species composition on the northeast shelf was largely accounted for by the unidirectional abundance gradient component (nestedness) of dissimilarity (Fig. 6b). This resulted from the apparent decrease (e.g., Alaska plaice, butterfly

sculpin, and great sculpin) and increase (e.g., walleye pollock, northern rock sole, and Pacific cod) in species abundances within survey sites in the area (n = 25) under the low sea ice regime. In the southern part of the middle shelf, however, the dissimilarity in community composition is mostly accounted for by the balanced changes in species abundances (turnover) (Fig 6c). The species pool accounted for 63.27% of the overall between-regime dissimilarity in community composition. A total of three fish taxa (i.e. walleye pollock, northern rock sole, and arrowtooth flounder) associated with the lwsic regime, were identified to be most influential in driving community composition changes, based on their significant average contributions to the overall dissimilarity (Table S5).

4. Discussion

The increasing and multi-faceted threats to marine biodiversity call for a better understanding of its long-term spatial patterns and temporal trends, especially within dynamic and climatically sensitive yet productive regions of the global ocean. Our study examined the contemporary distributions of taxonomic biodiversity aspects of marine communities on the continental shelf of the Eastern Bering Sea (EBS) and identified the importance of environmental covariates in modulating temporal and spatial patterns of local alpha- and beta-diversity. The use of actual species observations to elucidate spatio-temporal changes in biodiversity over the past 29 years enabled the identification of geographically distinct biodiversity refugial zones. These areas provided safe havens for marine species in the EBS under on-going climate changes as evident from the high species richness and stability in community compositions within these regions.

Additionally, the biodiversity refugia showed modest correspondence with climatically stable regions in the EBS over the past 29 years. Such spatial overlap between refugial features potentially supports the persistence of elevated marine biodiversity and species compositional similarity in these areas under recent climatic changes. Nonetheless, it is worth noting that these biodiversity refugia were also situated in areas of unstable climatic conditions, suggesting

339 that potential processes other than climate buffering are crucial in the formation of these
340 features. This further underpinned the importance of validation as an essential component of
341 the climate change refugia conservation cycle (Morelli et al., 2016) and ecosystem-based
342 management strategies to ensure adaptive and more effective responses in protecting
343 biodiversity and high-value resources (Barrows et al., 2020).

344 Refugia are indispensable for facilitating the persistence of components of biodiversity
345 under changing climates over certain ecological time scales (Keppel et al., 2012). In the EBS,
346 two latitudinally distinct refugia were identified on the middle shelf (50-100 m). Both areas
347 persisted through spatial and temporal variability in environmental and climatic conditions over
348 the last three decades. The formation of refugia may be linked to biophysical processes that
349 enhance productivity at these sites. One of the refugial zones straddles the transition zone
350 between the outer and middle domains on the southern shelf, a region of elevated summer
351 productivity due to the presence of structural fronts (Sambrotto et al., 2008). Similarly, the
352 north refugium is situated on the outer portion of the middle shelf and extends slightly past the
353 transition zone onto the outer shelf, a region where elevated production rates are fueled by
354 intense spring ice-edge blooms (Lomas et al., 2012; Stabeno et al., 2012). Hence, the high
355 summer primary productivity in these areas likely supports the high species richness in these
356 refugia. Moreover, the higher productivity in the north (58-60°N) relative to the south sector
357 of the middle shelf (Lomas et al., 2012) could account for higher percent frequencies of species
358 in the former than in the latter. High productivity may also explain the counterintuitive overlap
359 between these refugial zones and areas of intensive fishing, particularly the southern refugia,
360 accumulating the highest area disturbed across gear types (Olson, 2019). High primary
361 productivity may cushion marine communities against the impacts of fishing, consistent with
362 the reported minimal long-term effects of fisheries on fish populations in the area (Olson, 2019).
363 In any case, our results highlight the relevance of biodiversity refugial zones for ecosystem-

364 based management approaches to maintain resilient fisheries and ecosystems under a rapidly
365 changing climate.

366 While the overall stability in community composition was similar in the two refugia,
367 the north refugium showed distinct patches of high compositional similarity. It suggests that
368 the community in this zone is comprised of species that have a particular affinity or close
369 association to low-temperature waters (e.g., snow crab, wattled eelpout, and polar six-rayed
370 star) and are therefore generally more abundant on the northern shelf (Rand and Logerwell,
371 2011). In the south refugium, the highest similarity in community composition occurred close
372 to the inner front separating the inner and middle shelves, decreasing eastward. The wind-
373 driven inner front serves as a region of protracted production and an obstacle to faunal
374 exchanges between the inner and middle shelves (Stabeno and Hunt, 2002), thus likely
375 promoting the retention of distinct species assemblages at both sides of the inner and middle
376 shelves proximal to the frontal boundary. Likewise, climatically stable areas in the southern
377 region of the middle shelf were smaller relative to the north, potentially accounting for a lower
378 similarity in the species community composition in the south refugium. Despite the differences
379 in biodiversity components between the two refugia, these zones harbored a persistently large
380 portion of the species pool providing shelter for marine taxa in this shelf community under
381 contemporary climatic changes and substantial fishing footprint (Olson, 2019).

382 Nonetheless, we recognize that changing biological interactions at the refugia could
383 also have fundamental ecological consequences under future environmental and climatic
384 changes. The dominance of large predatory fish taxa (i.e. walleye pollock, Pacific cod, and
385 flathead sole) in the refugial zones, particularly in the north refugium, could significantly alter
386 predatory and competitive interactions within the existing community. For instance, gadoid
387 predation exerts top-down control of snow crab (*Chionoecetes opilio*) abundance in subarctic
388 and Arctic seas (Orensanz et al., 2005; Boudreau et al., 2011; Burgos et al., 2013). Similarly,

the intensified competition among predators for space and resources in high-density areas can also modify ecosystem-wide trophic linkages and prey resource dynamics (Hunsicker et al., 2013; Matassa et al., 2018). Therefore, effective adaptation strategy focusing on the conservation of climate change refugia can benefit from further incorporation of biological interactions into the framework (Kavousi, 2019), albeit our current understanding of many of these biotic interactions remains inadequate.

Our analysis of the effects of environmental factors on biodiversity is consistent with earlier studies on the impacts of sea ice dynamics on contemporary and future spatial distributions of marine species in the study area (Mueter and Litzow, 2008; Alabia et al., 2018; Alabia et al., 2020). The overall effect of winter sea ice concentration on species richness and community composition varied spatially. During periods of low sea ice concentration, the cold pool structure retracts north (Stabeno et al., 2012), allowing an extensive movement of species throughout the study area (Mueter and Litzow, 2008). This condition could facilitate foraging migrations of warm-affinity taxa to the more productive waters in the north sector of the middle shelf. The enhanced species movement responses, especially for large fish species (e.g., walleye pollock, arrowtooth flounder, and northern rock sole), under the lwsic regime increase the local species richness while promoting the biotic homogenization of local communities. Thus, resulting in increased similarity in species between periods of high and low winter sea ice conditions. In contrast, during the hwsic regime, the high species richness was limited to the southern part of the EBS. In the EBS, a sub-surface summer thermal layer associated with seasonal sea ice (Hunt et al., 2011), known as the cold pool, largely regulates species movement (Wyllie-Echeverria and Wooster, 1998). The cold pool feature is characterized by low bottom temperatures (< 2°C) that extend south to the southeastern shelf during periods of extensive winter sea ice coverage (Stabeno et al., 2012), posing an effective barrier to the movement of cold-intolerant species across the different domains and sectors of the continental shelf. This

results in the observed decrease in average regional alpha diversity over much of the middle shelf during the high winter sea ice periods.

Finally, in light of the rapid ecological transformations of high-latitude environments due to climate change and extreme events (e.g., marine heatwaves, atmospheric disturbances), it is all the more imperative to better understand the dynamics of potential refugial zones. In particular, continually assimilating the most recent and larger pool of biodiversity data into the analyses can better evaluate the capacity of refugial zones to cushion against emerging and multifaceted threats. We also recognized that bottom trawl survey data primarily target demersal fisheries, which may result in the under-representation of pelagic taxa in our analyses. Future incorporation of a larger species pool from pelagic habitats could offer further, more holistic insights into the nature of biodiversity refugial zones when that information becomes available. Additionally, adopting a gradient-based perspective of climate change refugia may improve the identification and protection of these areas, recognizing the difference in rates at which various biodiversity components will respond to climate change (Hannah et al., 2014; Morelli et al., 2020). Recent studies have shown that even marine protected areas in temperate regions were unable to forestall the heatwave-induced changes in the fish community structure (Freedman et al., 2020) and future climate change-driven decline in benthic species (Weinert et al., 2020). More than ever, climate-driven and intensified phenomena exacerbate the already tremendous challenge of biodiversity conservation, hence emphasizing the importance of identification and management of potential marine climate change and biodiversity refugia, ideally within a progressive context (Morelli et al., 2020).

Acknowledgments

We thank the various agencies that provided the datasets used for these analyses, in particular the Resource Assessment and Conservation Engineering Division at the Alaska Fisheries Science Center, NOAA. This work is supported by Japan's national programs on the Arctic

region, Arctic Challenge for Sustainability (ArCS) (JPMXD1300000000) and ArCS II (JPMXD1420318865), funded by Japan's Ministry of Education, Culture, Sports, Science, and Technology (MEXT). IDA received additional funding support from the Hokkaido University's function enhancement fund, Hokkaido University Arctic Initiative for Future Earth and SDGs.

References

Abdi, A. M., Boke-Olén, N., Jin, H., Eklundh, L., Tagesson, T., Lehsten, V., and Ardö, J. 2019. First assessment of the plant phenology index (PPI) for estimating gross primary productivity in African semi-arid ecosystems. International Journal of Applied Earth Observation and Geoinformation, 78: 249-260.

Alabia, I. D., García Molinos, J., Saitoh, S.-I., Hirawake, T., Hirata, T., and Mueter, F. J. 2018. Distribution shifts of marine taxa in the Pacific Arctic under contemporary climate changes. Diversity and Distributions, 24: 1583-1597.

Alabia, I. D., Molinos, J. G., Saitoh, S.-I., Hirata, T., Hirawake, T., and Mueter, F. J. 2020. Multiple facets of marine biodiversity in the Pacific Arctic under future climate. Science of The Total Environment, 744: 140913.

Ashcroft, M. B. 2010. Identifying refugia from climate change. Journal of Biogeography, 37: 1407-1413.

Ashcroft, M. B., Gollan, J. R., Warton, D. I., and Ramp, D. 2012. A novel approach to quantify and locate potential microrefugia using topoclimate, climate stability, and isolation from the matrix. Global Change Biology, 18: 1866-1879.

Assis, J., Coelho, N. C., Lamy, T., Valero, M., Alberto, F., and Serrão, E. Á. 2016. Deep reefs are climatic refugia for genetic diversity of marine forests. Journal of Biogeography, 43: 833-844.

Baker, M. R., and Hollowed, A. B. 2014. Delineating ecological regions in marine systems: Integrating physical structure and community composition to inform spatial

management in the eastern Bering Sea. Deep Sea Research Part II: Topical Studies in Oceanography, 109: 215-240.

Ban, N. C., Pressey, R. L., and Weeks, S. 2012. Conservation Objectives and Sea-Surface Temperature Anomalies in the Great Barrier Reef. Conservation Biology, 26: 799-809.

Ban, S. S., Alidina, H. M., Okey, T. A., Gregg, R. M., and Ban, N. C. 2016. Identifying potential marine climate change refugia: A case study in Canada's Pacific marine ecosystems. Global Ecology and Conservation, 8: 41-54.

Barbier, E. B. 2017. Marine ecosystem services. Current Biology, 27: R507-R510.

Barceló, C., Ciannelli, L., and Brodeur, R. D. 2018. Pelagic marine refugia and climatically sensitive areas in an eastern boundary current upwelling system. Global Change Biology, 24: 668-680.

Barrows, C. W., Ramirez, A. R., Sweet, L. C., Morelli, T. L., Millar, C. I., Frakes, N., Rodgers, J., et al. 2020. Validating climate-change refugia: empirical bottom-up approaches to support management actions. Frontiers in Ecology and the Environment, 18: 298-306.

Baselga, A. 2013. Separating the two components of abundance-based dissimilarity: balanced changes in abundance vs. abundance gradients. Methods in Ecology and Evolution, 4: 552-557.

Baselga, A., and Orme, C. D. L. 2012. betapart: an R package for the study of beta diversity. Methods in Ecology and Evolution, 3: 808-812.

Baumgartner, J. B., Esperón-Rodríguez, M., and Beaumont, L. J. 2018. Identifying in situ climate refugia for plant species. Ecography, 41: 1850-1863.

Boudreau, S. A., Anderson, S., and Worm, B. 2011. Top-down interactions and temperature control of snow crab abundance in the northwest Atlantic Ocean. Marine Ecology Progress Series, 429: 169-183.

488 Burgos, J., Ernst, B., Armstrong, D., and Orensanz, J. 2013. Fluctuations in Range and
489 Abundance of Snow Crab (Chionoecetes Opilio) from the Eastern Bering Sea: What
490 Role for Pacific Cod (Gadus Macrocephalus) Predation? Bulletin of Marine Science,
491 89: 57-81.
492 Burrows, M. T., Schoeman, D. S., Buckley, L. B., Moore, P., Poloczanska, E. S., Brander, K.
493 M., Brown, C., et al. 2011. The Pace of Shifting Climate in Marine and Terrestrial
494 Ecosystems. Science, 334: 652-655.
495 Cáceres, M. D., and Legendre, P. 2009. Associations between species and groups of sites:
496 indices and statistical inference. Ecology, 90: 3566-3574.
497 Cavanagh, R. D., Broszeit, S., Pilling, G. M., Grant, S. M., Murphy, E. J., and Austen, M. C.
498 2016. Valuing biodiversity and ecosystem services: a useful way to manage and
499 conserve marine resources? Proceedings of the Royal Society B: Biological Sciences,
500 283: 20161635.
501 Coachman, L. K. 1986. Circulation, water masses, and fluxes on the southeastern Bering Sea
502 shelf. Continental Shelf Research, 5: 23-108.
503 Danielson, S., Eisner, L., Weingartner, T., and Aagaard, K. 2011. Thermal and haline
504 variability over the central Bering Sea shelf: Seasonal and interannual perspectives.
505 Continental Shelf Research, 31: 539-554.
506 De Cáceres, M., Legendre, P., and Moretti, M. 2010. Improving indicator species analysis by
507 combining groups of sites. Oikos, 119: 1674-1684.
508 Duffy-Anderson, J. T., Stabeno, P. J., Siddon, E. C., Andrews, A. G., Cooper, D. W., Eisner,
509 L. B., Farley, E. V., et al. 2017. Return of warm conditions in the southeastern Bering
510 Sea: Phytoplankton - Fish. PLoS ONE, 12: e0178955.
511 Eisner, L. B., Gann, J. C., Ladd, C., D. Cieciel, K., and Mordy, C. W. 2016. Late summer/early
512 fall phytoplankton biomass (chlorophyll a) in the eastern Bering Sea: Spatial and

513 temporal variations and factors affecting chlorophyll a concentrations. Deep Sea
514 Research Part II: Topical Studies in Oceanography, 134: 100-114.
515 Eisner, L. B., Napp, J. M., Mier, K. L., Pinchuk, A. I., and Andrews, A. G. 2014. Climate-
516 mediated changes in zooplankton community structure for the eastern Bering Sea. Deep
517 Sea Research Part II: Topical Studies in Oceanography, 109: 157-171.
518 Freedman, R. M., Brown, J. A., Caldow, C., and Caselle, J. E. 2020. Marine protected areas do
519 not prevent marine heatwave-induced fish community structure changes in a temperate
520 transition zone. Scientific Reports, 10: 21081.
521 Genner, M. J., Sims, D. W., Southward, A. J., Budd, G. C., Masterson, P., McHugh, M., Rendle,
522 P., et al. 2010. Body size-dependent responses of a marine fish assemblage to climate
523 change and fishing over a century-long scale. Global Change Biology, 16: 517-527.
524 Hannah, L., Flint, L., Syphard, A. D., Moritz, M. A., Buckley, L. B., and McCullough, I. M.
525 2014. Fine-grain modeling of species' response to climate change: holdouts, stepping-
526 stones, and microrefugia. Trends in Ecology & Evolution, 29: 390-397.
527 Hirawake, T., and Hunt, G. L. 2020. Impacts of unusually light sea-ice cover in winter 2017-
528 2018 on the northern Bering Sea marine ecosystem – An introduction. Deep Sea
529 Research Part II: Topical Studies in Oceanography: 104908.
530 Hollowed, A. B., Bax, N., Beamish, R., Collie, J., Fogarty, M., Livingston, P., Pope, J., et al.
531 2000. Are multispecies models an improvement on single-species models for
532 measuring fishing impacts on marine ecosystems? ICES Journal of Marine Science, 57:
533 707-719.
534 Hooidonk, R. V., Maynard, J., Maynard, J., and Planes, S. 2013. Temporary refugia for coral
535 reefs in a warming world. Nature Climate Change, 3: 508-511.

536 Hunsicker, M. E., Ciannelli, L., Bailey, K. M., Zador, S., and Stige, L. C. 2013. Climate and
537 Demography Dictate the Strength of Predator-Prey Overlap in a Subarctic Marine
538 Ecosystem. PLoS ONE, 8: e66025.
539 Hunt, J. G. L., Coyle, K. O., Eisner, L. B., Farley, E. V., Heintz, R. A., Mueter, F., Napp, J. M.,
540 et al. 2011. Climate impacts on eastern Bering Sea foodwebs: a synthesis of new data
541 and an assessment of the Oscillating Control Hypothesis. ICES Journal of Marine
542 Science, 68: 1230-1243.
543 Isaak, D. J., Young, M. K., Luce, C. H., Hostetler, S. W., Wenger, S. J., Peterson, E. E., Ver
544 Hoef, J. M., et al. 2016. Slow climate velocities of mountain streams portend their role
545 as refugia for cold-water biodiversity. Proceedings of the National Academy of
546 Sciences, 113: 4374.
547 Jost, L., Chao, A., and Chazdon, R. 2010. Compositional similarity and#² (beta) diversity.
548 Kapsenberg, L., and Cyronak, T. 2019. Ocean acidification refugia in variable environments.
549 Global Change Biology, 25: 3201-3214.
550 Kavousi, J. 2019. Biological interactions: The overlooked aspects of marine climate change
551 refugia. Global Change Biology, 25: 3571-3573.
552 Keppel, G., Mokany, K., Wardell-Johnson, G. W., Phillips, B. L., Welbergen, J. A., and Reside,
553 A. E. 2015. The capacity of refugia for conservation planning under climate change.
554 Frontiers in Ecology and the Environment, 13: 106-112.
555 Keppel, G., Van Niel, K. P., Wardell-Johnson, G. W., Yates, C. J., Byrne, M., Mucina, L.,
556 Schut, A. G. T., et al. 2012. Refugia: identifying and understanding safe havens for
557 biodiversity under climate change. Global Ecology and Biogeography, 21: 393-404.
558 Krebs, C. J. 2014. Similarity Coefficients and Cluster Analysis. *In* Ecological methodology,
559 pp. 486-527. Benjamin/Cummings, Menlo Park, Calif.

Lomas, M. W., Moran, S. B., Casey, J. R., Bell, D. W., Tiahlo, M., Whitefield, J., Kelly, R. P., et al. 2012. Spatial and seasonal variability of primary production on the Eastern Bering Sea shelf. Deep Sea Research Part II: Topical Studies in Oceanography, 65-70: 126-140.

Lourenço, C. R., Zardi, G. I., McQuaid, C. D., Serrão, E. A., Pearson, G. A., Jacinto, R., and Nicastro, K. R. 2016. Upwelling areas as climate change refugia for the distribution and genetic diversity of a marine macroalga. Journal of Biogeography, 43: 1595-1607.

Malhi, Y., Franklin, J., Seddon, N., Solan, M., Turner, M. G., Field, C. B., and Knowlton, N. 2020. Climate change and ecosystems: threats, opportunities and solutions. Philosophical Transactions of the Royal Society B: Biological Sciences, 375: 20190104.

Matassa, C. M., Ewanchuk, P. J., and Trussell, G. C. 2018. Cascading effects of a top predator on intraspecific competition at intermediate and basal trophic levels. Functional Ecology, 32: 2241-2252.

Morelli, T. L., Barrows, C. W., Ramirez, A. R., Cartwright, J. M., Ackerly, D. D., Eaves, T. D., Ebersole, J. L., et al. 2020. Climate-change refugia: biodiversity in the slow lane. Frontiers in Ecology and the Environment, 18: 228-234.

Morelli, T. L., Daly, C., Dobrowski, S. Z., Dulen, D. M., Ebersole, J. L., Jackson, S. T., Lundquist, J. D., et al. 2016. Managing Climate Change Refugia for Climate Adaptation. PLoS ONE, 11: e0159909-e0159909.

Morelli, T. L., Maher, S. P., Lim, M. C. W., Kastely, C., Eastman, L. M., Flint, L. E., Flint, A. L., et al. 2017. Climate change refugia and habitat connectivity promote species persistence. Climate Change Responses, 4: 8.

Mueter, F. J., and Litzow, M. A. 2008. Sea ice retreat alters the biogeography of the Bering Sea continental shelf. Ecological Applications, 18: 309-320.

584 Oksanen, J., Blanchet FG, Friendly M, Kindt R, Legendre P, McGlinn D, Minchin PR, et al.
585 2019. vegan: Community Ecology Package. R package version 2.5-6. https://CRAN.R-
586 project.org/package=vegan.
587 Olson, J. 2019. Area Disturbed by Trawl Fishing Gear in the Eastern Bering Sea. In: Siddon,
588 E. and Zador S., Eds. (2019) Ecosystem Status Report 2019: Eastern Bering Sea. North
589 Pacific Fishery Management Council, 605 W. 4th Avenue, Suite 306, Anchorage, AK
590 99301, pp. 162-164
591 Orensanz, J. M., Ernest, B., Armstrong, D., Stabeno, P., and Livingston, P. 2005. Contraction
592 of the geographic range of distribution of snow crab (Chionoecetes opilio) in the eastern
593 Bering Sea: An environmental ratchet?
594 Ortiz, I., Aydin, K., Hermann, A. J., Gibson, G. A., Punt, A. E., Wiese, F. K., Eisner, L. B., et
595 al. 2016. Climate to fish: Synthesizing field work, data and models in a 39-year
596 retrospective analysis of seasonal processes on the eastern Bering Sea shelf and slope.
597 Deep Sea Research Part II: Topical Studies in Oceanography, 134: 390-412.
598 Overland, J. E., and Stabeno, P. J. 2004. Is the climate of the Bering Sea warming and affecting
599 the ecosystem? Eos, Transactions American Geophysical Union, 85: 309-312.
600 Pinheiro, H. T., Bernardi, G., Simon, T., Joyeux, J.-C., Macieira, R. M., Gasparini, J. L., Rocha,
601 C., et al. 2017. Island biogeography of marine organisms. Nature, 549: 82-85.
602 Planque, B. 2016. Projecting the future state of marine ecosystems, “la grande illusion”? ICES
603 Journal of Marine Science, 73: 204-208.
604 Provan, J. 2013. The effects of past, present and future climate change on range-wide genetic
605 diversity in northern North Atlantic marine species. Frontiers of Biogeography, 5.
606 Rand, K. M., and Logerwell, E. A. 2011. The first demersal trawl survey of benthic fish and
607 invertebrates in the Beaufort Sea since the late 1970s. Polar Biology, 34: 475-488.

608 Rodionov, S. N. 2006. Use of prewhitening in climate regime shift detection. Geophysical
609 Research Letters, 33: L12707.
610 Sala, E., and Knowlton, N. 2006. Global Marine Biodiversity Trends. Annual Review of
611 Environment and Resources, 31: 93-122.
612 Sambrotto, R. N., Mordy, C., Zeeman, S. I., Stabeno, P. J., and Macklin, S. A. 2008. Physical
613 forcing and nutrient conditions associated with patterns of Chl a and phytoplankton
614 productivity in the southeastern Bering Sea during summer. Deep Sea Research Part II:
615 Topical Studies in Oceanography, 55: 1745-1760.
616 Selig, E. R., Turner, W. R., Troëng, S., Wallace, B. P., Halpern, B. S., Kaschner, K., Lascelles,
617 B. G., et al. 2014. Global Priorities for Marine Biodiversity Conservation. PLoS ONE,
618 9: e82898.
619 Springer, A. M., McRoy, C. P., and Flint, M. V. 1996. The Bering Sea Green Belt: shelf-edge
620 processes and ecosystem production. Fisheries Oceanography, 5: 205-223.
621 Stabeno, P. J., and Bell, S. W. 2019. Extreme Conditions in the Bering Sea (2017–2018):
622 Record-Breaking Low Sea-Ice Extent. Geophysical Research Letters, 46: 8952-8959.
623 Stabeno, P. J., Duffy-Anderson, J. T., Eisner, L. B., Farley, E. V., Heintz, R. A., and Mordy,
624 C. W. 2017. Return of warm conditions in the southeastern Bering Sea: Physics to
625 fluorescence. PLoS ONE, 12: e0185464.
626 Stabeno, P. J., and Hunt, G. L. 2002. Overview of the Inner Front and Southeast Bering Sea
627 Carrying Capacity Programs. Deep Sea Research Part II: Topical Studies in
628 Oceanography, 49: 6157-6168.
629 Stabeno, P. J., Kachel, N. B., Moore, S. E., Napp, J. M., Sigler, M., Yamaguchi, A., and Zerbini,
630 A. N. 2012. Comparison of warm and cold years on the southeastern Bering Sea shelf
631 and some implications for the ecosystem. Deep Sea Research Part II: Topical Studies
632 in Oceanography, 65–70: 31-45.

633 Stauffer, G. 2004. NOAA protocols for groundfish bottom trawl surveys of the nation's fishery
634 resources. Technical Memorandum NMFS-F/SPO-65, U.S. Department of Commerce,
635 NOAA, Washington, D.C., USA.
636 Stevenson, D. E., and Hoff, G. R. 2009. Species identification confidence in the eastern Bering
637 Sea (1982–2008). 46 pp. pp.
638 Stevenson, D. E., and Lauth, R. R. 2019. Bottom trawl surveys in the northern Bering Sea
639 indicate recent shifts in the distribution of marine species. Polar Biology, 42: 407-421.
640 Stewart, J. R., Lister, A. M., Barnes, I., and Dalén, L. 2010. Refugia revisited: individualistic
641 responses of species in space and time. Proceedings of the Royal Society B: Biological
642 Sciences, 277: 661-671.
643 Storlazzi, C. D., Cheriton, O. M., van Hooidonk, R., Zhao, Z., and Brainard, R. 2020. Internal
644 tides can provide thermal refugia that will buffer some coral reefs from future global
645 warming. Scientific Reports, 10: 13435.
646 Sydeman, W. J., Poloczanska, E., Reed, T. E., and Thompson, S. A. 2015. Climate change and
647 marine vertebrates. Science, 350: 772.
648 Tittensor, D. P., Mora, C., Jetz, W., Lotze, H. K., Ricard, D., Berghe, E. V., and Worm, B.
649 2010. Global patterns and predictors of marine biodiversity across taxa. Nature, 466:
650 1098-1101.
651 Weinert, M., Mathis, M., Kröncke, I., Pohlmann, T., and Reiss, H. 2020. Climate change effects
652 on Marine Protected Areas: projected decline of benthic species in the North Sea.
653 Marine Environmental Research: 105230.
654 Wessel, P., Smith, W. H. F., Scharroo, R., Luis, J., and Wobbe, F. 2013. Generic Mapping
655 Tools: Improved Version Released. Eos, Transactions American Geophysical Union,
656 94: 409-410.

Wood, S. 2006. Generalized Additive Models: An Introduction with R, Chapman and Hall/CRC, Boca Raton, Florida.

Wyllie-Echeverria, T., and Wooster, W. S. 1998. Year-to-year variations in Bering Sea ice cover and some consequences for fish distributions. Fisheries Oceanography, 7: 159-170.

662 **Table 1.** Average percent frequency of annual occurrence of representative taxa inside (37 stations) and outside (339 stations) of the designated

663 refugia zone over the 29 years of the study period. Species with higher frequencies within the refugia are highlighted in bold.

Common name	Scientific name	Percent frequency			
		Inside refugia			Outside refugia
		South	North	Overall	
Walleye pollock	*Gadus chalcogrammus*	42.96	56.66	99.63	96.23
Pacific cod	*Gadus macrocephalus*	42.78	56.10	98.88	95.04
Basketstar	*Gorgonocephalus eucnemis*	41.66	54.89	96.55	55.11
Snow crab	*Chionoecetes opilio*	36.63	56.48	93.10	68.80
Flathead sole	*Hippoglossoides elassodon*	41.94	50.51	92.45	73.41
Alaska plaice	*Pleuronectes quadrituberculatus*	41.47	45.67	87.14	64.33
Tanner crab	*Chionoecetes bairdi*	41.01	42.40	83.41	61.40
Polar six-rayed star	*Leptasterias polaris*	30.20	52.10	82.29	30.38
Northern rock sole	*Lepidopsetta polyxystra*	34.11	43.62	77.73	67.10
Alaska skate	*Bathyraja parmifera*	32.62	44.45	77.07	69.81
Wattled eelpout	*Lycodes palearis*	28.15	47.72	75.86	32.27
Pacific halibut	*Hippoglossus stenolepis*	32.53	35.79	68.31	71.59
Yellowfin sole	*Limanda aspera*	42.87	23.95	66.82	66.30
Great sculpin	*Myoxocephalus polyacanthocephalus*	26.75	34.86	61.60	42.56
Circumboreal toad crab	*Hyas coarctatus*	33.92	26.75	60.67	41.82
Purple-orange sea star	*Asterias amurensis*	38.30	20.32	58.62	64.42
Arrowtooth flounder	*Atheresthes stomias*	19.66	33.74	53.40	48.91
Sturgeon poacher	*Podothecus accipenserinus*	37.09	16.31	53.40	57.13
Pribilof whelk	*Neptunea pribiloffensis*	10.07	42.03	52.10	33.26

664

Table 2. Generalized additive mixed model outputs for alpha and beta-diversity. Estimated degrees of freedom, F-values (t-values for factor terms) obtained for each environmental correlate and asterisks represent significance levels at *p* less than 0.05 (*), 0.01 (**) or 0.001(***). Model performance were assessed based on adjusted R^2 and Akaike Information Criterion (AIC) values.

Models	**Predictors**	**Abbreviation**	**Estimated degrees of freedom (edf)**	**t/F-value**	**Adj R^2**	**AIC**
α-diversity					0.458	49941
	year	yr		46.76***		
	longitude,latititude	x,y	27.79	36.59**		
	bottom temperature gradient	btg	1.95	14.22**		
	surface temperature gradient	stg	1.90	9.92***		
	bottom depth	bdep	1.91	5.70*		
	maximum summer sea surface temperature (SST)	$ssst_{max}$	1.90	4.05*		
	winter sea ice concentration	wsic	1.97	15.57***		
	distance to the nearest coast	$dist_{coast}$	1.88	3.27*		
β-diversity					0.150	-21493
	year	yr		−15.86***		
	longitude,latititude	x,y	24.85	10.69***		
	bottom temperature gradient	btg	1.00	5.12*		
	surface temperature gradient	stg				
	bottom depth	bdep	1.91	9.09**		
	maximum summer SST	$ssst_{max}$				
	winter sea ice concentration	wsic	1.92	31.44***		
	distance to the nearest coast	$dist_{coast}$	1.92	5.83**		

Figure legends

Figure 1. Temporal trends in (a) regionally (polygon in inset map) averaged species richness and (b) change in species composition (Sorensen dissimilarity) with vertical bars representing one positive and negative standard deviation. Gray broken lines correspond to the climatological average of alpha (24.48, 1990-2018) and temporal beta-diversity (0.26, 1991-2018). Blue lines show the least-squares linear regressions of each biodiversity metric on year.

Figure 2. Spatially-interpolated distributions of (a) mean α-diversity (rescaled to 0–1), (b) mean within-site temporal community similarity (presented as the inverse of Sorensen dissimilarity), (c) the resultant refugia index computed as the product of mean α- and mean within-site temporal β-diversity, and (d) climatic stability based on the sum of neutral (largely unchanged trend) pixels for winter sea ice concentration and seasonal sea surface temperatures. Regions in blue did not have any neutral pixels; areas in red contained neutral pixels in all three variables. The polygons denote the identified refugia zones (refugia index value of 0.31, 90% quantile of refugia index) and the broken lines correspond to the 50 and 100 m isobaths.

Figure 3. Number of species inside the refugia and their biogeographic affinity between the north (21 stations) and south (16 stations) refugia (inset map).

Figure 4. Significant partial effects of environmental variables (a-f) on alpha diversity (species richness) and (g-j) beta diversity (Sorensen dissimilarity) predicted from a generalized additive mixed model. The solid lines are estimated mean effects, the gray shaded areas are the 95% point-wise confidence intervals, and 0 represents the reference for a null effect (broken lines). Ticks along the x-axis are points at which observations were obtained between 1990 and 2018.

692 **Figure 5.** Spatial structures of averaged annual alpha diversity during (a) the high (1990-1999;
693 2008-2013), (b) low (2000-2007; 2014-2018) winter sea ice (wsic) regimes in the
694 Eastern Bering Sea, and (c) the species richness difference between the contrasting
695 regimes. Broken lines correspond to the 50 and 100 m isobaths.
696 **Figure 6.** Spatial patterns of (a) abundance-based Bray-Curtis dissimilarity and (b-c) respective
697 components between high and low wsic regimes. Broken lines correspond to the 50 and
698 100 m isobaths.

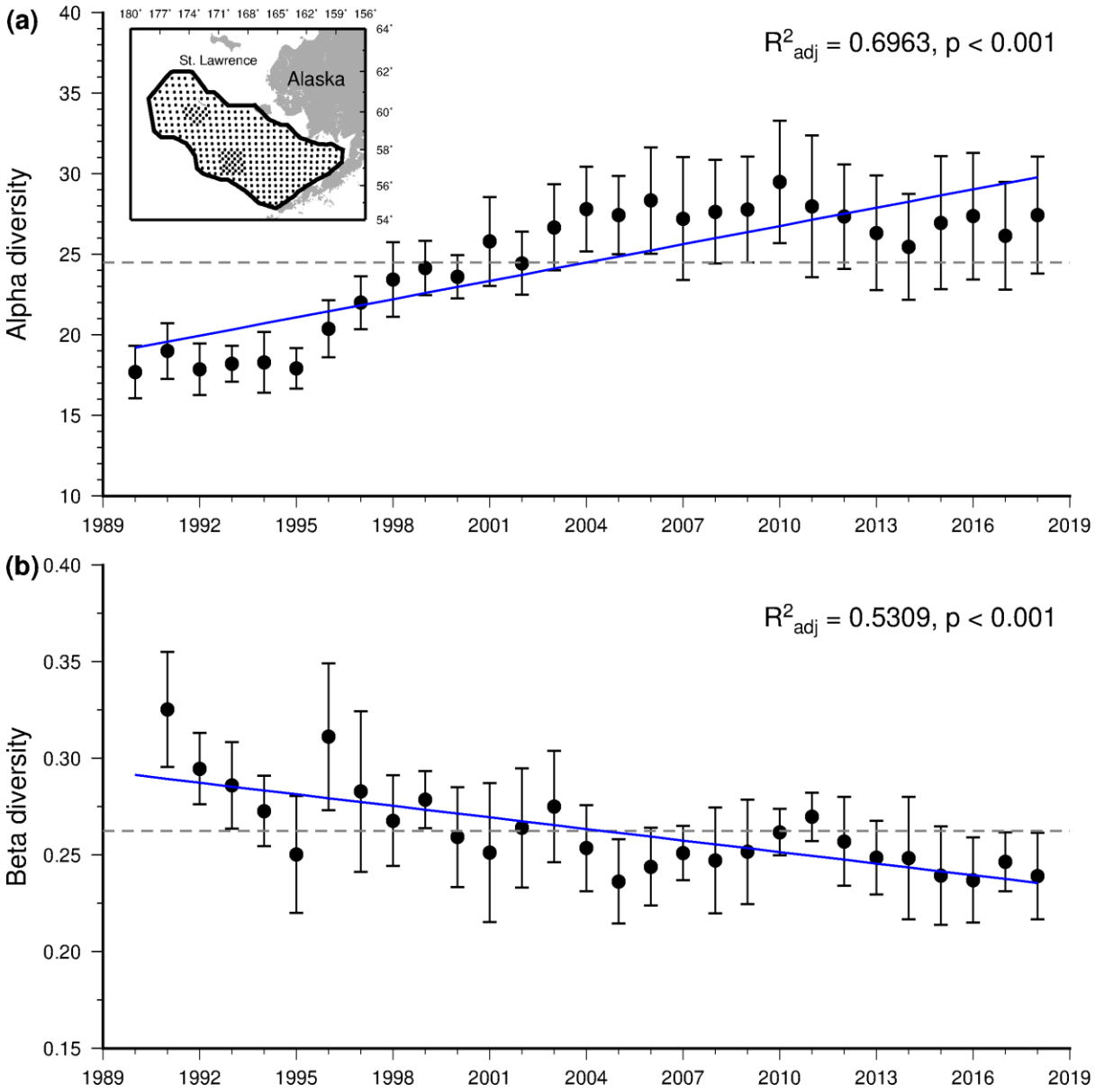

Figure 1. Temporal trends in (a) regionally (polygon in inset map) averaged species richness and (b) change in species composition (Sorensen dissimilarity) with vertical bars representing one positive and negative standard deviation. Gray broken lines correspond to the climatological average of alpha (24.48, 1990-2018) and temporal beta-diversity (0.26, 1991-2018). Blue lines show the least-squares linear regressions of each biodiversity metric on year.

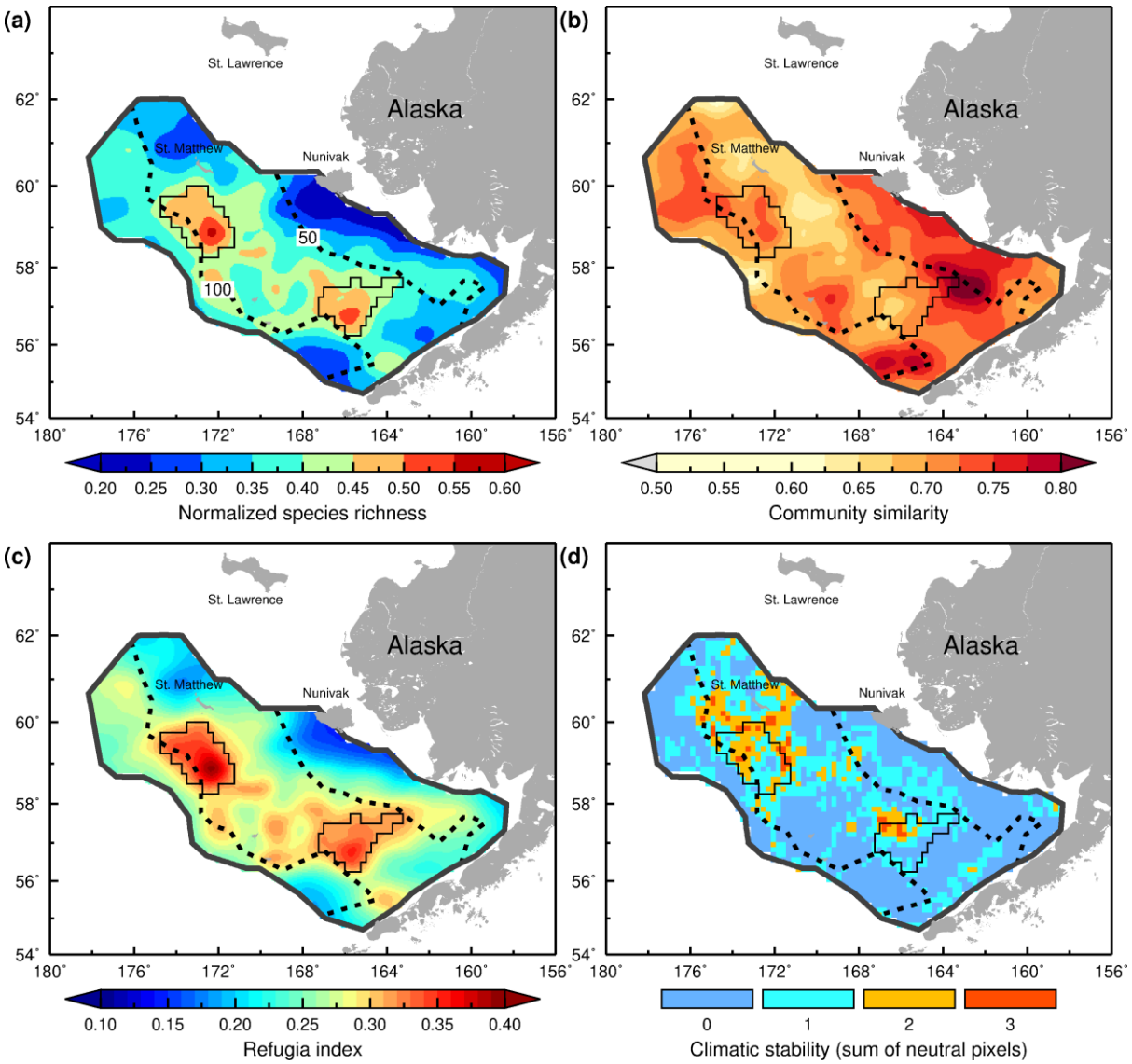

Figure 2. Spatially-interpolated distributions of (a) mean α-diversity (rescaled to 0–1), (b) mean within-site temporal community similarity (presented as the inverse of Sorensen dissimilarity), (c) the resultant refugia index computed as the product of mean α- and mean within-site temporal β-diversity, and (d) climatic stability based on the sum of neutral (largely unchanged trend) pixels for winter sea ice concentration and seasonal sea surface temperatures. Regions in blue did not have any neutral pixels; areas in red contained neutral pixels in all three variables. The polygons denote the identified refugia zones (refugia index value of 0.31, 90% quantile of refugia index) and the broken lines correspond to the 50 and 100 m isobaths.

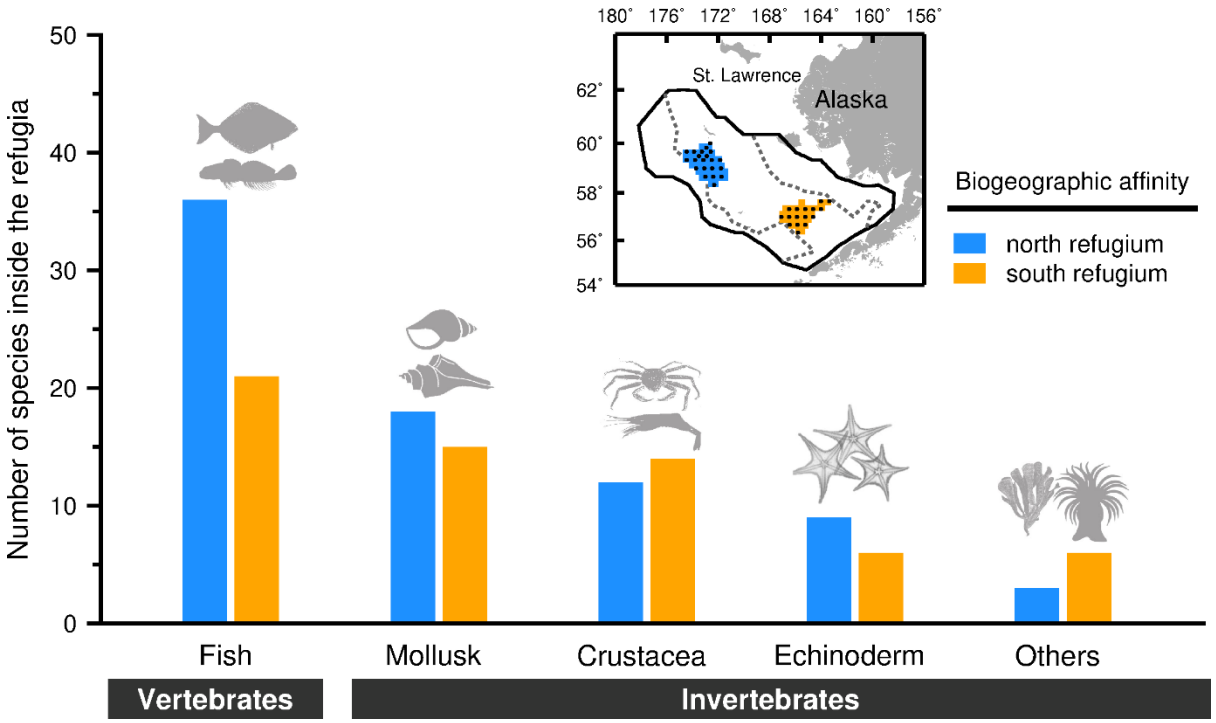

712 **Figure 3.** Number of species inside the refugia and their biogeographic affinity between the

713 north (21 stations) and south (16 stations) refugia (inset map).

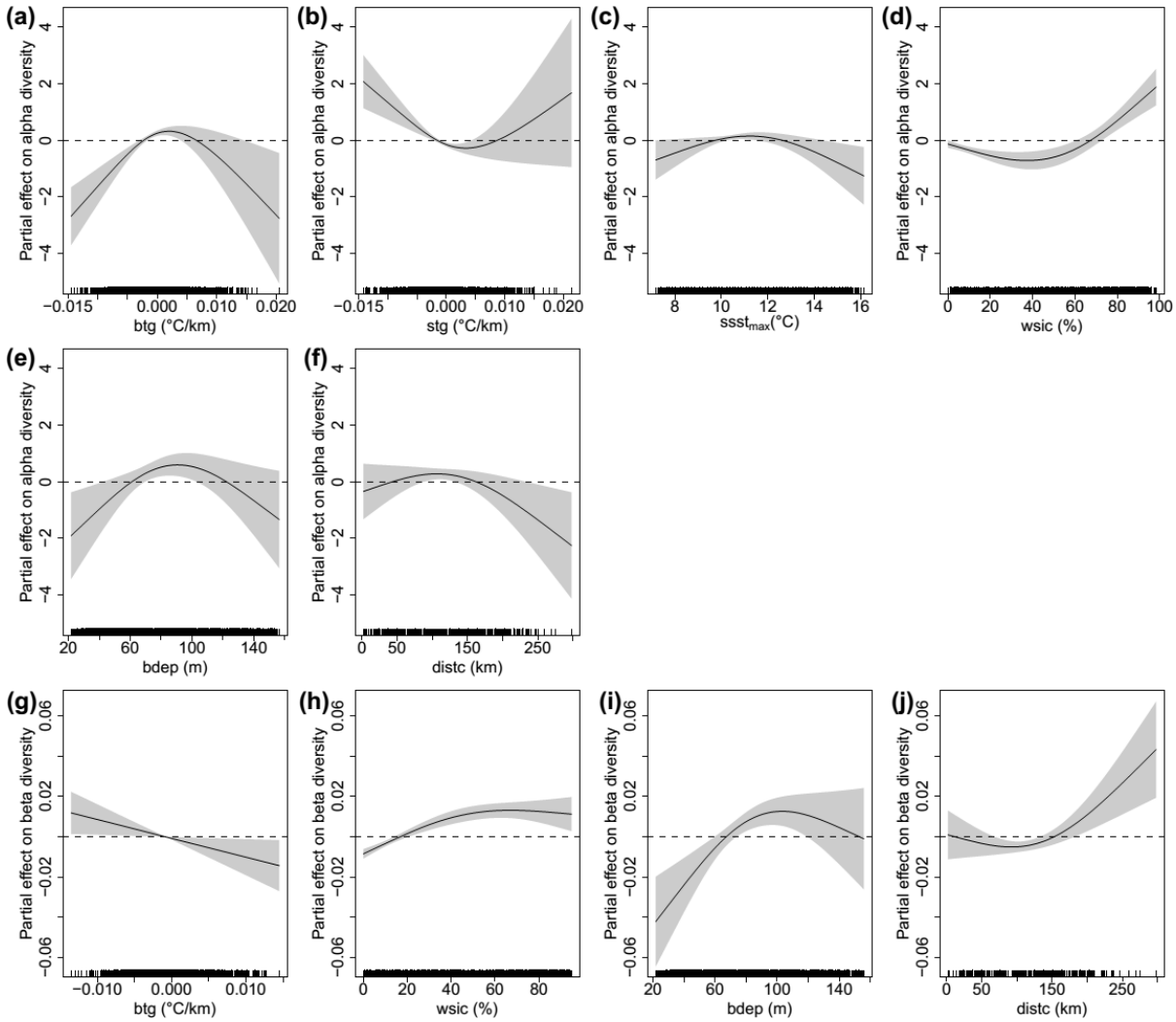

Figure 4. Significant partial effects of environmental variables (a-f) on alpha diversity (species richness) and (g-j) beta diversity (Sorensen dissimilarity) predicted from a generalized additive mixed model. The solid lines are estimated mean effects, the gray shaded areas are the 95% point-wise confidence intervals, and 0 represents the reference for a null effect (broken lines). Ticks along the x-axis are points at which observations were obtained between 1990 and 2018.

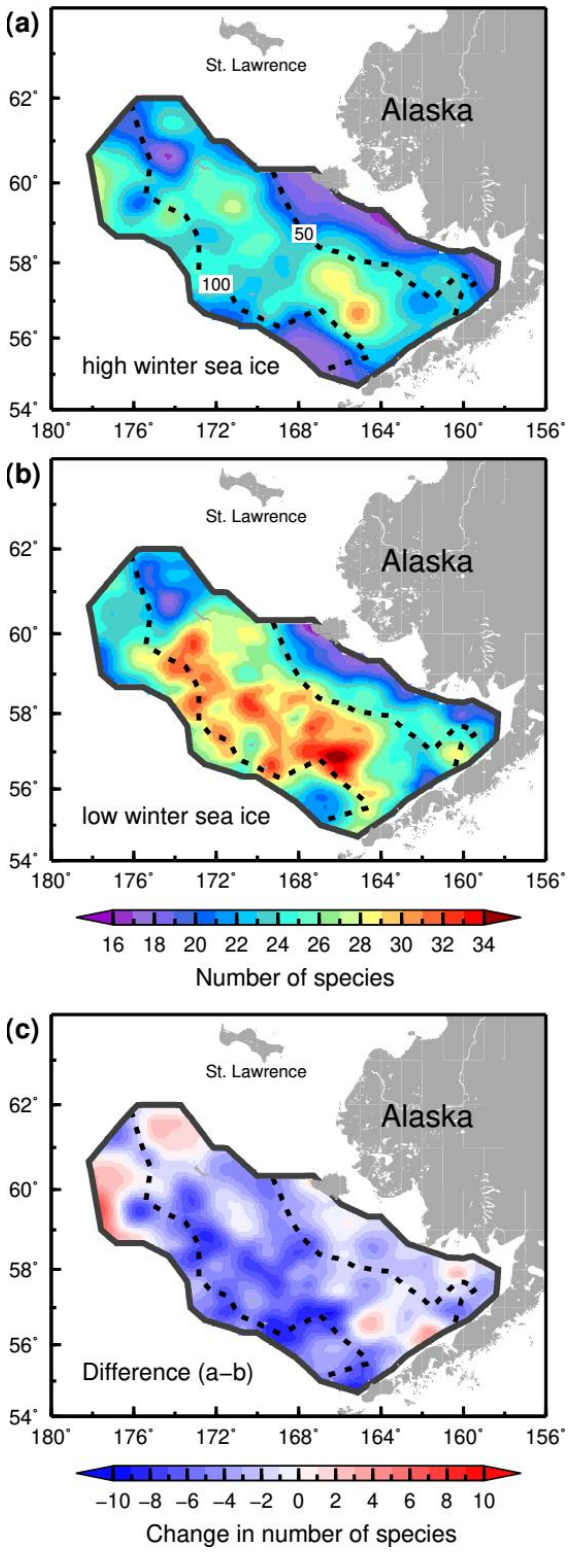

719 **Figure 5.** Spatial structures of averaged annual alpha diversity during (a) the high (1990-1999;
720 2008-2013), (b) low (2000-2007; 2014-2018) winter sea ice (wsic) regimes in the Eastern
721 Bering Sea, and (c) the species richness difference between the contrasting regimes. Broken
722 lines correspond to the 50 and 100 m isobaths.

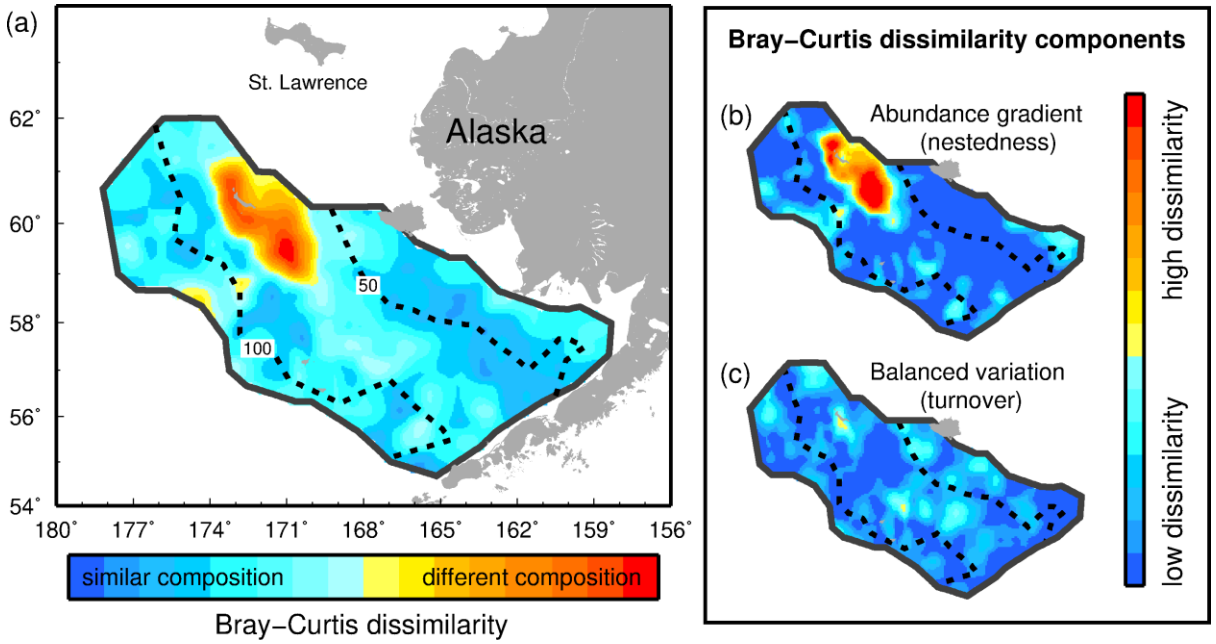

723 **Figure 6.** Spatial patterns of (a) abundance-based Bray-Curtis dissimilarity and (b-c) respective
724 components between high and low wsic regimes. Broken lines correspond to the 50 and 100 m
725 isobaths.